

Full paper

Detection of non-joint areas tiny strain and anti-interference voice recognition by micro-cracked metal thin film



Chunfeng Wang^{a,b,1}, Jing Zhao^{a,b,1}, Chuang Ma^{a,b}, Junlu Sun^{a,b}, Li Tian^{a,b}, Xiaoyi Li^a, Fangtao Li^a, Xun Han^a, Chuntai Liu^b, Changyu Shen^b, Lin Dong^{a,b,*}, Jin Yang^{c,*}, Caofeng Pan^{a,*}

^a Beijing Institute of Nanoenergy and Nanosystems, Chinese Academy of Sciences; National Center for Nanoscience and Technology (NCNST), Beijing 100083, China

^b The Key Laboratory of Materials Processing and Mold of Ministry of Education, School of Materials Science and Engineering, School of Physical Engineering, Zhengzhou University, Zhengzhou 450001, China

^c Department of Optoelectronic Engineering, Chongqing University, Chongqing 400044, China

ARTICLE INFO

Keywords:

Strain sensor
Micro-cracks Metal thin film
Healthcare monitoring
Anti-interference voice recognition

ABSTRACT

The poor detecting limit and attenuated sensitivity to tiny strain of a strain sensor retard their development toward practical applications ranging from wearable electronics, human healthcare monitoring to smart sensing system. Here, a strain sensor with high sensitivity to tiny strain, high flexibility, fast response and good stability is developed utilizing the micro-cracked metal thin film based on a novel working principle of combining the overlap mode with tunnel effect of the adjacent cracks. Monitoring of human motions and physiological signals as well as anti-interference voice recognition based on the sensor is demonstrated, showing its potential applications in wearable electronics, human healthcare monitoring and smart sensing system.

1. Introduction

By converting mechanical motions into electrical signals based on changes in capacitance and resistance, the strain sensor carries significant importance in wearable electronics, smart sensing system and personalized health monitoring system [1–6]. In order to work effectively and comfortably, the strain sensor must have high flexibility and stretchability so that it is able to laminate comfortably and noninvasively onto the human skin while maintaining the abilities of high sensitivity, high gauge factor, fast response and good stability. Especially, the gauge factor (GF) defined as $GF = \frac{\Delta R/R_0}{\epsilon}$ ($\Delta R/R_0$ is the relative change in resistance and ϵ is the corresponding mechanical strain) is a key metric to evaluate the performance of the strain sensor. By virtue of advances in materials and mechanics designs, many groups have been dedicated to the advancement of the strain sensor over the past decade. Yamada et al. demonstrated a highly stretchable strain sensor *via* the thin films of aligned single-walled carbon nanotubes showing a 280% strain but low GF of 0.82 [7]. Ryu et al. showed that the oriented carbon nanotube fibers grown on the Ecoflex substrate can be stretched by over 900% while having a GF of up to 47 [8]. Li et al. transferred ultrathin graphene onto the PDMS substrate to achieve a GF of 1037 at 2% strain [9]. Zaretski et al. utilized metallic nano-

islands on graphene to achieve a highly sensitive strain sensor with GF of 1335 at 1% strain [10]. Despite these advances, the sensor for detecting tiny strain (strain < 1%, such as strain of human non-joint areas and throat vibrations) with the attributes of high sensitivity, high GF, fast response and good stability is still very limited. On the other hand, a conspicuous inconvenience of the current voice recognition system is that the system cannot discriminate the signals of the owners from the troublemakers. For example, the microphone/loudspeaker will simultaneously broadcast all of the sounds it can capture without distinguishing the signals and the background noise. Thus, the anti-interference voice recognition system is urgently desired and will find important applications in smart home, portable electronics and military security [11–15].

Cracks in conductive materials are considered as defects to be avoided in general, leading to resistance increases or even failure of the conductive materials. But if we consider this problem from another perspective, the cracks in conductive materials may provide an approach to realize ultrahigh sensitivity of the strain sensor because of its straightforward disconnect-reconnection feature upon stretching-releasing. Therefore, ultrasensitive strain sensors utilizing micro-cracked platinum and gold thin film have been achieved [16,17]. But these works mainly focus on study of the working principle and

* Corresponding authors.

E-mail addresses: ldong@zzu.edu.cn (L. Dong), yangjin@cqu.edu.cn (J. Yang), cspan@binn.cas.cn (C. Pan).

¹ Chunfeng Wang and Jing Zhao contributed equally to this work.

performance optimization of the device, further research such as applications is still urgently required.

Here, we demonstrate an ultrasensitive strain sensor by depositing a layer of gold/titanium (Au/Ti) thin film on the PDMS substrate followed by pre-stretching for generating the micro-cracks in the metal thin film. The working mechanism of the micro-cracked strain sensor is based on the coupling of overlap mode and tunnel effect of the adjacent cracks. The micro-cracked strain sensor is lightweight, cost-effective and scalable with the attributes of highly flexibility, high sensitivity to tiny strain and vibration (strain < 1%), high GF (~5000 in the range of 0–1% strain), fast response (137 ms) and good stability (over 700 cycles). As a demonstration, the strain sensor can be mounted on the human skin to detecting tiny strain of human non-joint areas, physiological pulse wave, canthus motion and any biological associated skin deformation, which is important to monitor the spirit status and physiological signals of one person. Meanwhile, spatial strain distribution on the dorsal side of one's hand when clench the fist can be achieved by extending the sensor to a multi-pixel array due to its simple and cost-effective fabrication process. More importantly, an anti-interference voice recognition system is demonstrated by attaching the sensor to one's throat to record his/her phonation signals with a piece of music as the background noise. In all, the ultrasensitive strain sensor offers a promising opportunity to smart home, wearable electronics, health monitoring systems and even military security.

2. Material and methods

2.1. Fabrication of micro-cracked metal thin film strain sensor

The fabrication process of the micro-cracked strain sensor is schematically illustrated in Fig. 1a. The PDMS substrate is prepared by solidifying the mixture of the elastomer and cross-linker (Sylgard 184, Dow Corning) with a weight ratio of 10:1 at 70 °C for 5 h. The

metal thin film including a layer of Ti (10 nm) and a layer of Au (50 nm) are deposited on the PDMS substrate *via* the electron beam evaporation (Denton Vacuum Explore 14) with a depositing rate of 1 Å/s under the chamber pressure of 2×10^{-6} Torr. Then the pre-stretch of 10% strain controlled by the 3D micromanipulation stages is applied to the sample for the formation of the micro-cracks. Cu fine wires are connected to both ends of the sample with silver paste after release of the pre-strain.

2.2. Fabrication of multi-pixel sensor array

As shown in Fig. 4a and Fig. S3, Supporting information, the first layer of metal thin film including a 10 nm layer of Ti and a 50 nm layer of Au with the design pattern is firstly deposited on the PDMS substrate by combining the shadow mask and electron beam evaporation. Subsequently, the pre-stretch of 10% strain controlled by the 3D micromanipulation stages is applied to the sample for the formation of the micro-cracks and then release. The second layer of metal thin film only including a 50 nm layer of Au as the top electrode is deposited *via* the electron beam evaporation. The PDMS insulating spacers array are placed at the cross-points between the top and bottom electrodes to avoid the leakage.

2.3. Characterization

The morphology of the metal thin film before and after pre-stretching characterized by the optical microscope (Zeiss Observer Z1) and the field-emission scanning electron microscope (SEM, FEI Nova NanoSEM 450). The electromechanical behavior of the sensor in Fig. 2 and Fig. 3 is recorded with the LCR meter (Agilent E4980A) with a sampling rate of 10 Hz. The electromechanical behavior of the sensor in Fig. 5 is recorded with the Stanford Research System (SR 570 low noise current amplifier equipped with DS 345 synthesized function

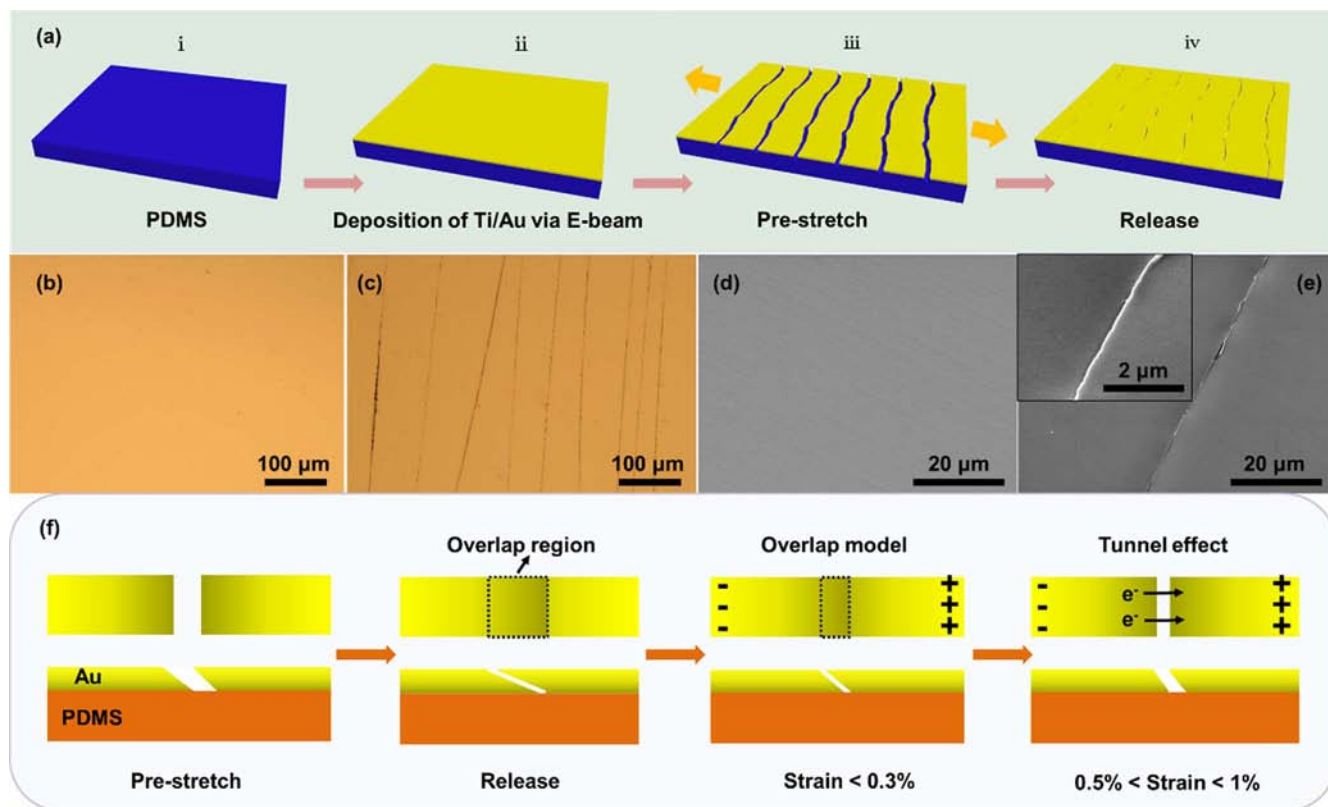


Fig. 1. Structure and working mechanism of the micro-cracked metal thin film strain sensor. (a) Schematic illustration of the micro-cracked strain sensor fabrication process. (b, c) Optical images of the metal thin film before and after pre-stretch at a level of 10% strain. (d, e) SEM images of the metal thin film before and after pre-stretch at a level of 10% strain. (f) The proposed working mechanism of the micro-cracked strain sensor.

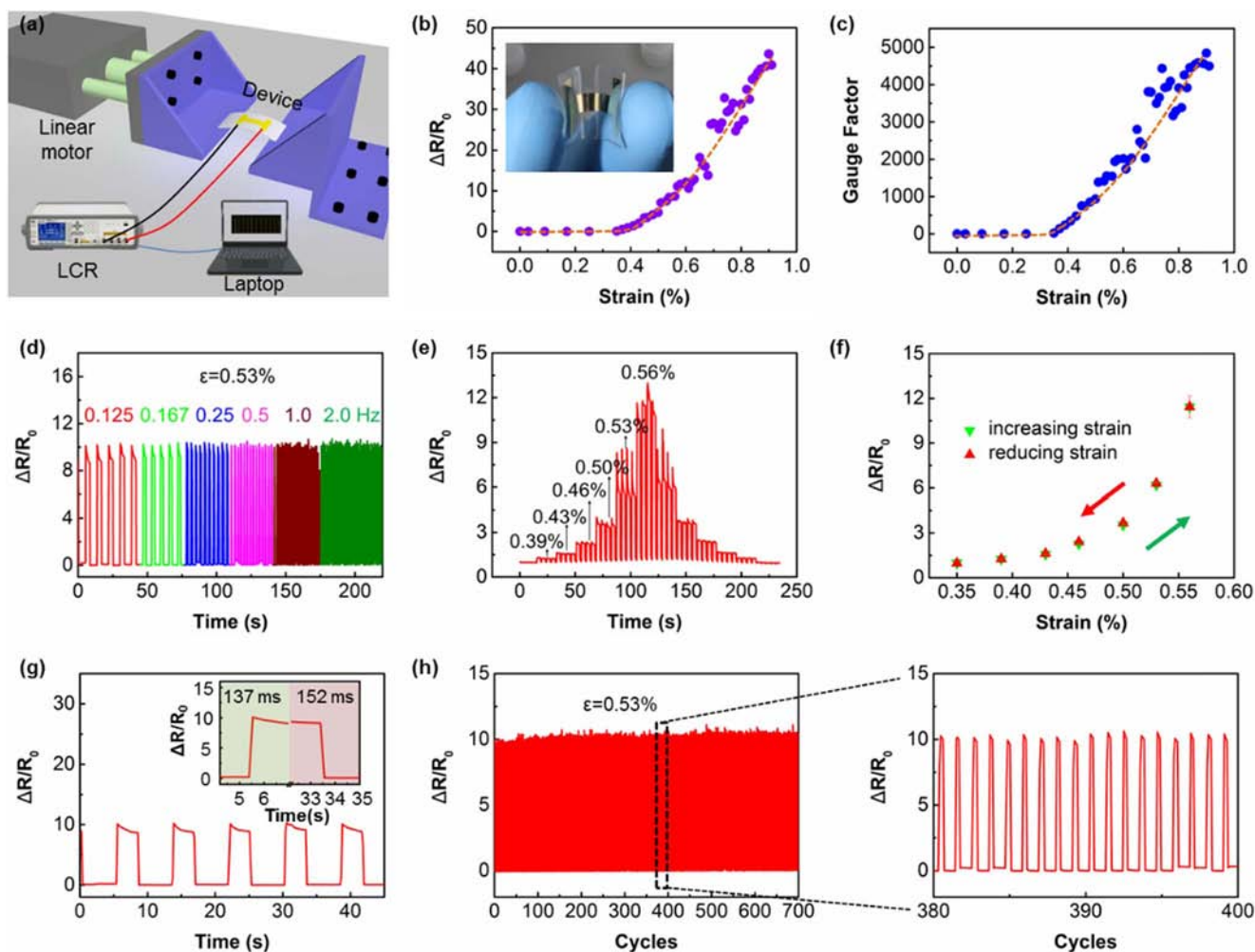


Fig. 2. Electromechanical characterizations of the micro-cracked metal thin film strain sensor. (a) Schematic illustration of the measurement setup for the electromechanical behaviors recording of the micro-cracked strain sensor. (b) Relative resistance changes of the micro-cracked strain sensor with a rising strain. Inset shows the photograph of a representative micro-cracked strain sensor. (c) Gain factor (GF) of the micro-cracked strain sensor under different strains. (d) Relative resistance response of the micro-cracked strain sensor as a function of the loading frequency at a strain of 0.53%. (e, f) The reversible resistance changes of the micro-cracked strain sensor under increasing and reducing strains. (g) Time response of the micro-cracked strain sensor. Inset shows the response times of 137 ms and 152 ms for rising and recovering, respectively. (h) Mechanical durability of the micro-cracked strain sensor under a strain of 0.53%.

generator) with a sampling rate of 10 kHz. The electromechanical behavior of the multi-pixel sensor array is recorded by using the multichannel current testing system (Keithley 2612B system source-meter combing with 3706A system switch/multimeter).

3. Results and discussion

As shown in the optical and SEM images of the sample in Fig. 1b–e, some parallel channel cracks perpendicular to the direction of pre-strain appear during the pre-stretch process and most of the cracks stay closed with the overlapped crack edges after the pre-strain is released, which is important for efficacious sensing of the device. The working principle of the micro-cracked strain sensor can be explained based on the coupling of overlap mode and tunnel effect [17,18], which is schematically illustrated in Fig. 1f. At the stage of small strains (strain < 0.3%), the resistance changes of the micro-cracked strain sensor can be ascribed to the changes of the overlap area between the adjacent cracks because the overlap resistance is much larger than the intralayer one of the metal thin film. The resistance of the sensor rises slowly with the decreasing overlap area of the adjacent cracks. Upon the further stretching (0.5% < strain < 1%), the adjacent cracks lost their contact, the resistance of the sensor is depending on the tunnel effect, which rises rapidly with the increasing displace of disconnection.

For the interval strain (0.3% ≤ strain ≤ 0.5%), the working mechanism can be explained by combination of the overlap mode and tunnel effect.

To characterize the electromechanical behaviors of the micro-cracked strain sensor, a liner motor is used to apply strains to the sensor and the corresponding resistance changes of the sensor are measured by the LCR instrumentation, as shown in Fig. 2a. The variation of the relative resistance ($\Delta R/R_0$) to the applied strain (calculation of the strain can be found in Fig. S1, Supporting information) is shown in Fig. 2b. Inset in Fig. 2b is the photograph of a representative sensor. The relative resistance change increases slowly in the beginning of the strain up to 0.35%, after which the increasing trend of $\Delta R/R_0$ becomes sharply with the applied strain, which can be explained well by the proposed working mechanism. Fig. 2c shows the gauge factor (GF) of the micro-cracked strain sensor under different strain situations. With the highest value of about 5000 at the strain range of 0–1%, the GF of the micro-cracked strain sensor is much higher than those previously reported mostly strain sensor based on graphite, graphene, nanowires and carbon nanotubes [19–24], which benefits from the disconnection/fracture mechanism of the metal thin film upon stretching. Considering the frequency-dependence of strain sensor is one of the major characteristics when utilized in the sensor fields [25], the resistance response of the micro-cracked strain sensor under repeated loading-unloading cycles of 0.53% strain at

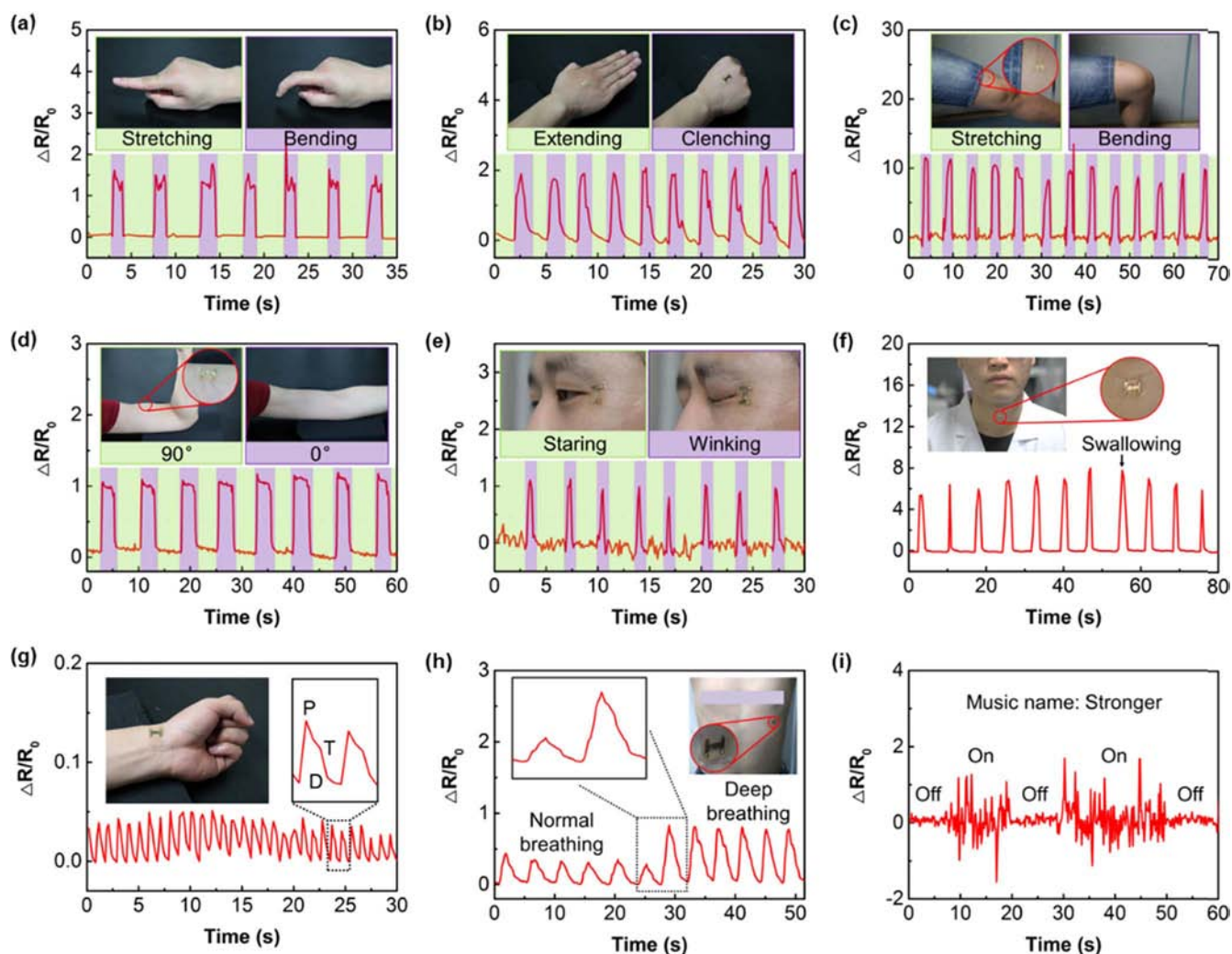


Fig. 3. Demonstration of the micro-cracked metal thin film strain sensor applications for detecting tiny strains. (a) The signal recording during the stretching-bending process of the finger with the micro-cracked strain sensor adhered on the finger non-joint area. (b) The signal recording during the extending-clenching process of the hand with the micro-cracked strain sensor mounted on the dorsal sides of the hand. (c) The signal recording during the stretching-bending process of the leg with the micro-cracked strain sensor adhered on the thigh. (d) Response to muscular tension and relaxation of the micro-cracked strain sensor by attaching it on the forearm. (e) The signal recording during the staring-winking process by attaching the micro-cracked strain sensor on the canthus. (f) Response to the swallowing behavior by attaching the micro-cracked strain sensor on the Adam's apple. (g) Output signal of the micro-cracked strain sensor when attached on wrist. Inset in the upper right is an enlarged view of one circle of the signal obtained, whose waveform comprise of three main parts, labeled as P-wave, T-wave and D-wave. (h) Human respiration monitoring when the micro-cracked strain sensor is placed on the chest. Inset in the upper left shows the enlarged view of a representative signal. (i) Response to the acoustic vibrations from a piece of music with the micro-cracked strain sensor on the surface of an earphone. Photos of the insets in a-h show the corresponding photographs for signals acquisition.

different frequencies is compared and shown in Fig. 2d and Fig. S2 of Supporting information. There are no obviously frequency-related peak-loss and hysteresis observed at the frequency range of 0.125–2 Hz, which demonstrates the stable and fast response of the sensor.

The reproducibility of sensing capacity of the micro-cracked strain sensor is investigated by applying the stepped strain to the sensor. Fig. 2e shows the relative resistance changes of the sensor under the increasing and decreasing strains with an excellent strain resolution of 0.03%. Fig. 2f is the resistance response of the sensor depending on the strain extracted from Fig. 2e, from which only the negligible hysteresis is observed, indicating the sensor behaves reversibly and nearly elastically because of the improved adhesion between the Au thin film and the PDMS substrate utilizing the Ti adhesive layer [26,27]. Fig. 2g and the enlarged view of the loading and unloading process in its inset show the response and relaxation times of the micro-cracked strain sensor is 137 ms and 152 ms, respectively. The mechanical durability of the micro-cracked strain sensor is shown in Fig. 2h. There is no obvious degradation of the sensing performance observed under a strain of 0.53% after 700 cycles, demonstrating the excellent roughness

and stability of the sensor.

The muscle contractions of human non-joint areas carry abundant information for medical diagnostics, rehabilitation training and health monitoring [28–30]. However, most of the previous works focus on the motion sensing of human joint areas such as the finger joints, elbows and knees [31–34], which probably due to their detecting limits and attenuated sensitivity to tiny strain. Here, the micro-cracked strain sensor can be used as wearable sensor to monitor the subtle motions of human non-joint areas such as extensor pollicis longus contraction, physiological pulse wave and canthus motion due to its high sensitivity to tiny strain, highly flexibility, lightweight and non-toxicity. The micro-cracked strain sensors are mounted comfortably on the human skins through the medical tapes. Fig. 3a shows the repeatable and stable resistance response of the sensor to the extensor pollicis longus contraction by attaching the sensor to the finger non-joint areas to measure the skin strain. The relative resistance changes significantly due to the deformation of muscle when the finger motion from stretch to bend. The inset in Fig. 3a shows the corresponding level when the finger stretches and bends. Similarly, the motion monitoring of the

dorsal muscle of opisthenar, quadriceps femoris of the leg and bicep of the arm can be demonstrated by attaching the sensors to the corresponding parts of the human body, as shown in Fig. 3b–d and their insets.

In addition, the micro-cracked strain sensor is capable of detecting any biological associated skin deformation for real-time monitoring of the spirit status and physiological signals of one person. For example, we attach the sensor at the corner of the eye and the throat to sense winking and swallowing movements, as shown in Fig. 3e, f and their insets. The resistance responses of staring and winking of the eye and the movement of the Adam's apple could be identified clearly, providing significant information about the spirit status of one person such as degree of fatigue, quality of sleep and sense of hunger. The real-time monitoring of the physiological pulse is desirable for early diagnosis of cardiovascular disease [35], which could be realized by attaching the sensors to the wrist and chest, respectively. The typical radial artery pulse waveform could be recorded precisely with two clearly distinguishable peaks corresponding to percussion wave (P) and diastolic wave (D) and a late systolic augmentation shoulder corresponding to tidal wave (T) as shown in Fig. 3g and its inset. Respiration, as another vital physiological signal, is achieved and presented in Fig. 3h and its inset. The different amplitudes of the signal peaks under normal and deep breathing condition indicates a potential application of the sensor for monitoring apnea in adults and sudden infant death syndrome [28,36]. At last, detection of tiny acoustic vibrations from music with resolved frequency and amplitude could be realized by attaching the sensor on the surface of an earphone, as shown in Fig. 3i.

The spatial strain distribution sensing of human skin is urgently required for the particular applications in epidermal electronics and human-machine interaction systems [37–39]. For this purpose, we fabricate a multi-pixel strain sensor array based on the micro-cracked metal thin film to map the spatial strain distribution of human skin by recording the relative resistance changes of every pixel simultaneously. Fig. 4a shows the schematic illustration of the multi-pixel sensor array (details of the fabrication process can be found in Section 2 and Fig. S3, Supporting information), in which the PDMS insulating spacers are used to avoid the leakage between the top and bottom electrodes. The photographs of a representative device is presented in Fig. 4b, exhibiting the highly flexibility of the device. Fig. 4c shows the demonstration of the sensor array for detecting the spatial strain distribution of the opisthenar when clench the fist. All strains of the opisthenar derived from the clench could be detected and reconstructed by the three-dimensional bars and the two-dimensional contour map as shown in

Fig. 4d and e, respectively, in which the resistance responses of different opisthenar areas with different levels of deformation could be clearly identified and precisely recorded.

A conspicuous inconvenience of the current voice recognition system is that the system cannot discriminate the signals of the owners from those of the troublemakers. For example, the microphone/loudspeaker will simultaneously broadcast all of the sounds it can capture without distinguishing the signals and the background noise. Thus, the anti-interference voice recognition system is urgently desired and will find important applications in smart home, portable electronics and even military security. To prove the capability of the micro-cracked strain sensor as an anti-interference microphone for voice recognition, we attach the sensor to a volunteer's throat to monitor the relative resistance changes caused by the tiny epidermis and muscle movements when the volunteer says different words and phrases with a piece of music as the background noise. As demonstrated in Fig. 5a–g and Movie S1–3, Supporting information, the sensor exhibits clearly distinguishable signal patterns corresponding to a series of phonations with excellent repeatability, superb anti-interference capability and high sensitivity. To further investigate its capability of anti-interference, we record the phonation signal of the sensor under series of volumes of the background noise, ranging from 81 dB (equivalent to busy street) to 103 dB (equivalent to subway train). As shown in Fig. 5h and Movie S4, Supporting information, the sensor still has a superb distinct and repeatable signal when the volunteer say the phrase “Welcome to China” even the volume of the noise is much higher than that of the signal so that the signal almost cannot be captured by the video camera, proving its powerful capability of anti-interference. Fig. 5i shows the screenshot of the anti-interference test.

Supplementary material related to this article can be found online at <http://dx.doi.org/10.1016/j.nanoen.2017.02.050>.

4. Conclusions

In summary, we have developed an ultrasensitive strain sensor based on the micro-cracked metal thin film, which is lightweight, cost-effective and scalable with the attributes of highly flexibility, high sensitivity to tiny strain and vibration, high gauge factor, fast response and good stability. For the practical applications, detection of tiny strain of human skin caused by muscle contraction and physiological pulse is firstly demonstrated. Subsequently, strain distribution sensing of human non-joint areas is achieved using the multi-pixel sensor matrix. Last but not least, an anti-interference voice recognition system

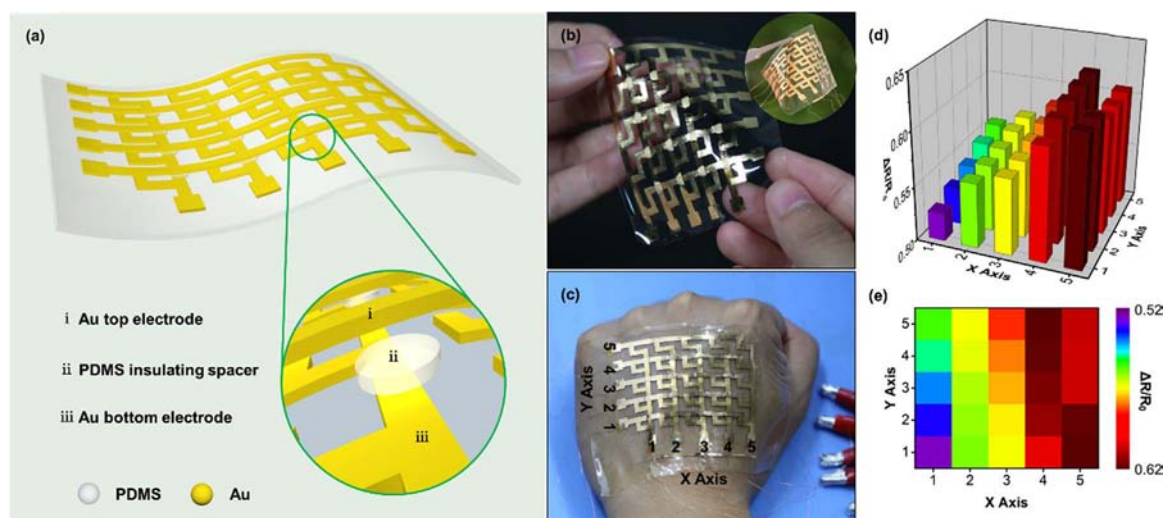


Fig. 4. Strain distribution detection by the multi-pixel array of the micro-cracked metal thin film strain sensor. (a) Structural design of the micro-cracked strain sensor array. (b) Photographs of the representative micro-cracked strain sensor array. (c) Photograph of the micro-cracked strain sensor array on the back of the hand for detecting strain distribution. (d, e) The recording strain distributions by the micro-cracked strain sensor array when clench the fist.

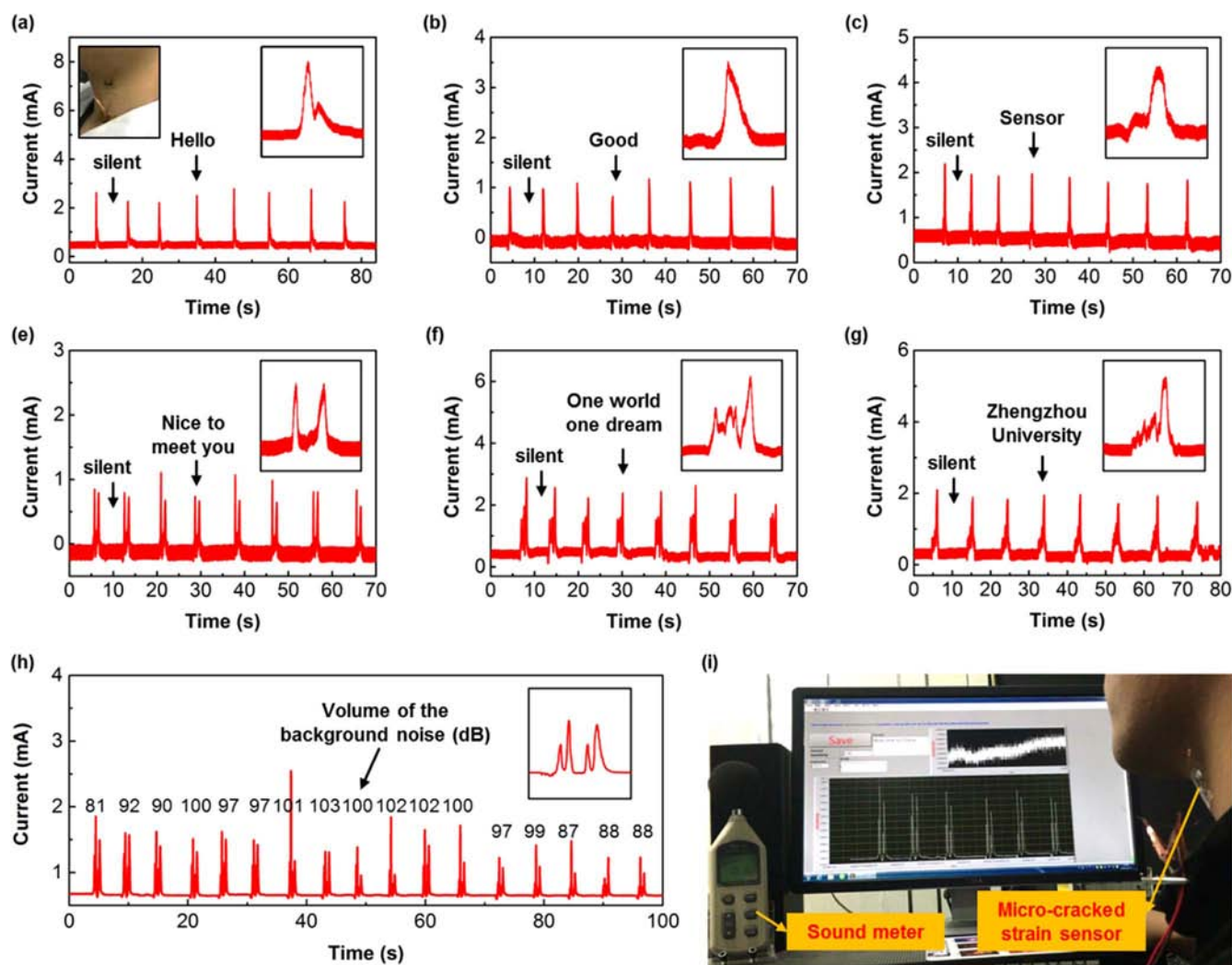


Fig. 5. Anti-interference voice recognition utilizing the micro-cracked metal thin film strain sensor. (a–h) Output signals of the micro-cracked strain sensor when saying different words with a piece of music as the background noise. Inset in the upper left of figure a shows the photo of the sensor adhered to the throat. Insets in the upper right of figure a–h show the enlarged views of the signals. (i) The screenshot of the anti-interference test.

is realized. This work is expected to pave the way to the potential applications of the micro-cracked strain sensor in smart home, health monitoring systems, wearable electronics and even military security.

Acknowledgements

The authors are thankful for support from National Natural Science Foundation of China (No. 51622205, 61675027, 61405040, 51432005, 61505010, 11674290 and 51502018), the support of national key R & D project from Minister of Science and Technology, China (2016YFA0202703), Beijing Natural Science Foundation (2164076), the "Thousand Talents" program of China for pioneering researchers and innovative teams, and Talent Project of Zhengzhou University (ZDGD13001) and Surface Engineering Key Lab of LIPCAST, Financial support from the program of China Scholarship Council (No. 201607040003).

Appendix A. Supplementary information

Supplementary data associated with this article can be found in the online version at: <http://dx.doi.org/10.1016/j.nanoen.2017.02.05>.

References

- [1] D.-H. Kim, N. Lu, R. Ma, Y.-S. Kim, R.-H. Kim, S. Wang, J. Wu, S.M. Won, H. Tao, A. Islam, K.J. Yu, T.-i. Kim, R. Chowdhury, M. Ying, L. Xu, M. Li, H.-J. Chung, H. Keum, M. McCormick, P. Liu, Y.-W. Zhang, F.G. Omenetto, Y. Huang, T. Coleman, J.A. Rogers, *Science* 333 (2011) 838–843.
- [2] Q. Zhang, L. Tan, Y. Chen, T. Zhang, W. Wang, Z. Liu, L. Fu, *Adv. Sci.* 3 (2016) 1600130.
- [3] T.Q. Trung, N.-E. Lee, *Adv. Mater.* 28 (2016) 4338–4372.
- [4] W. Weng, P. Chen, S. He, X. Sun, H. Peng, *Angew. Chem. Int. Ed.* 55 (2016) 6140–6169.
- [5] A. Chortos, J. Liu, Z. Bao, *Nat. Mater.* 15 (2016) 937–950.
- [6] C. Larson, B. Peele, S. Li, S. Robinson, M. Totaro, L. Beccai, B. Mazzolai, R. Shepherd, *Science* 351 (2016) 1071–1074.
- [7] T. Yamada, Y. Hayamizu, Y. Yamamoto, Y. Yomogida, A. Izadi-Najafabadi, D.N. Futaba, K. Hata, *Nat. Nanotechnol.* 6 (2011) 296–301.
- [8] S. Ryu, P. Lee, J.B. Chou, R. Xu, R. Zhao, A.J. Hart, S.-G. Kim, *ACS Nano* 9 (2015) 5929–5936.
- [9] X. Li, T. Yang, Y. Yang, J. Zhu, L. Li, F.E. Alam, X. Li, K. Wang, H. Cheng, C.T. Lin, *Adv. Funct. Mater.* 26 (2016) 1322–1329.
- [10] A.V. Zaretski, S.E. Root, A. Savchenko, E. Molokanova, A.D. Printz, L. Jibril, G. Arya, M. Mercola, D.J. Lipomi, *Nano Lett.* 16 (2016) 1375–1380.
- [11] Y. Wei, S. Chen, Y. Lin, Z. Yang, L. Liu, *J. Mater. Chem. C* 3 (2015) 9594–9602.
- [12] Y. Wang, L. Wang, T. Yang, X. Li, X. Zang, M. Zhu, K. Wang, D. Wu, H. Zhu, *Adv. Funct. Mater.* 24 (2014) 4666–4670.
- [13] X. Wang, Y. Gu, Z. Xiong, Z. Cui, T. Zhang, *Adv. Mater.* 26 (2014) 1336–1342.
- [14] Y. Wang, T. Yang, J. Lao, R. Zhang, Y. Zhang, M. Zhu, X. Li, X. Zang, K. Wang, W. Yu, *Nano Res.* 8 (2015) 1627–1636.
- [15] J. Yang, J. Chen, Y. Liu, W. Yang, Y. Su, Z.L. Wang, *ACS Nano* 8 (2014) 2649–2657.
- [16] D. Kang, P.V. Pikhitsa, Y.W. Choi, C. Lee, S.S. Shin, L. Piao, B. Park, K.-Y. Suh, T.-i. Kim, M. Choi, *Nature* 516 (2014) 222–226.

- [17] T. Yang, X. Li, X. Jiang, S. Lin, J. Lao, J. Shi, Z. Zhen, Z. Li, H. Zhu, *Mater. Horiz.* 3 (2016) 248–255.
- [18] Q. Liu, J. Chen, Y. Li, G. Shi, *ACS Nano* 10 (2016) 7901–7906.
- [19] B.-C. Zhang, H. Wang, Y. Zhao, F. Li, X.-M. Ou, B.-Q. Sun, X.-H. Zhang, *Nanoscale* 8 (2016) 2123–2128.
- [20] E. Roh, B.-U. Hwang, D. Kim, B.-Y. Kim, N.-E. Lee, *ACS Nano* 9 (2015) 6252–6261.
- [21] Y.R. Jeong, H. Park, S.W. Jin, S.Y. Hong, S.S. Lee, J.S. Ha, *Adv. Funct. Mater.* 25 (2015) 4228–4236.
- [22] J.T. Muth, D.M. Vogt, R.L. Truby, Y. Mengüç, D.B. Kolesky, R.J. Wood, J.A. Lewis, *Adv. Mater.* 26 (2014) 6307–6312.
- [23] M. Amjadi, K.U. Kyung, I. Park, M. Sitti, *Adv. Funct. Mater.* 26 (2016) 1678–1698.
- [24] X. Liao, Z. Zhang, Q. Liao, Q. Liang, Y. Ou, M. Xu, M. Li, G. Zhang, Y. Zhang, *Nanoscale* 8 (2016) 13025–13032.
- [25] J. Kuang, L. Liu, Y. Gao, D. Zhou, Z. Chen, B. Han, Z. Zhang, *Nanoscale* 5 (2013) 12171–12177.
- [26] S. Gong, W. Schwalb, Y. Wang, Y. Chen, Y. Tang, J. Si, B. Shirinzadeh, W. Cheng, *Nat. Commun.* 5 (2014) 3132.
- [27] S.J. Park, J. Kim, M. Chu, M. Khine, *Adv. Mater. Technol.* 1 (2016) 1600053.
- [28] C. Wang, X. Li, E. Gao, M. Jian, K. Xia, Q. Wang, Z. Xu, T. Ren, Y. Zhang, *Adv. Mater.* 28 (2016) 6640–6648.
- [29] J. Yang, J. Chen, Y. Su, Q. Jing, Z. Li, F. Yi, X. Wen, Z. Wang, Z.L. Wang, *Adv. Mater.* 27 (2015) 1316–1326.
- [30] L.Y. Chen, B.C.K. Tee, A.L. Chortos, G. Schwartz, V. Tse, D.J. Lipomi, H.S.P. Wong, M.V. McConnell, Z. Bao, *Nat. Commun.* 5 (2014) 5028.
- [31] G.-H. Lim, N.-E. Lee, B. Lim, *J. Mater. Chem. C* 4 (2016) 5642–5647.
- [32] J.J. Park, W.J. Hyun, S.C. Mun, Y.T. Park, O.O. Park, *A.C.S. Appl. Mater. Interfaces* 7 (2015) 6317–6324.
- [33] P.K. Yang, L. Lin, F. Yi, X. Li, K.C. Pradel, Y. Zi, C.I. Wu, H. He Jr, Y. Zhang, Z.L. Wang, *Adv. Mater.* 27 (2015) 3817–3824.
- [34] J.C. Yeo, J. Yu, M. Shang, K.P. Loh, C.T. Lim, *Small* 12 (2016) 1593–1604.
- [35] Z. Lou, S. Chen, L. Wang, K. Jiang, G. Shen, *Nano Energy* 23 (2016) 7–14.
- [36] Y. Cheng, R. Wang, J. Sun, L. Gao, *Adv. Mater.* 27 (2015) 7365–7371.
- [37] R. Bao, C. Wang, L. Dong, R. Yu, K. Zhao, Z.L. Wang, C. Pan, *Adv. Funct. Mater.* 25 (2015) 2884–2891.
- [38] W.-H. Yeo, Y.-S. Kim, J. Lee, A. Ameen, L. Shi, M. Li, S. Wang, R. Ma, S.H. Jin, Z. Kang, Y. Huang, J.A. Rogers, *Adv. Mater.* 25 (2013) 2773–2778.
- [39] C. Wang, R. Bao, K. Zhao, T. Zhang, L. Dong, C. Pan, *Nano Energy* 14 (2015) 364–371.



Chunfeng Wang is currently a Ph.D. candidate majoring in Materials Processing Engineering at School of Materials Science and Engineering, Zhengzhou University. He has joined in the group of Professor Caofeng Pan at Beijing Institute of Nanoenergy and Nanosystems, Chinese Academy of Sciences as a visiting student since 2013. His research focuses on nanowire optoelectronic devices and stretchable electronics.



Jing Zhao is currently a M.S. candidate majoring in Materials Science at School of Materials Science and Engineering, Zhengzhou University. She has joined in the group of Prof. Caofeng Pan as a visiting student at Beijing Institute of Nanoenergy and Nanosystems, Chinese Academy of Sciences since 2015. Her main research interests are flexible stretchable electronic devices and their applications in future e-skin, advanced robotics and healthcare monitoring.



Junlu Sun received his B.S. degree in Materials Science and Engineering from Zhengzhou University in 2014. He is currently studying in Materialogy as a master at Zhengzhou University. He has joined in the group of Professor Caofeng Pan at Beijing Institute of Nanoenergy and Nanosystems, CAS as a visiting student since 2015. His research focuses on the fields of flexible thin film perovskite solar cells and piezotronic/piezophototronic effects of nano-devices.



Chuang Ma received his B.S. degree in Materials Science and Engineering from Zhengzhou University in 2015. He is currently pursuing a M.S. degree in Material Science at Zhengzhou University. He has joined in the group of Professor Caofeng Pan at Beijing Institute of Nanoenergy and Nanosystems, CAS as a visiting student since 2015. His research focuses on semiconductor nanomaterials and their application in photoelectric devices.



Li Tian is currently a M.S. candidate majoring in Materials Science at School of Materials Science and Engineering, Zhengzhou University. She has joined in the group of Professor Caofeng Pan at Beijing Institute of Nanoenergy and Nanosystems, Chinese Academy of Sciences as a visiting student since 2016. His research focuses on optoelectronic devices based on 2D atomic monolayer materials.



Xiaoyi Li is currently a Ph.D. candidate in the school of Materials Science and Engineering, Tsinghua University. He is also an exchange student of the Beijing Institute of Nanoenergy and Nanosystems, Chinese Academy of Science from 2012. He received his B.S. degrees in Southeast University. His research interests include nanoscale semiconductor materials, piezo-photonics and nano-generators.



Fangtao Li is currently a Ph.D. candidate at School of Mathematics and Physics, University of Science and Technology Beijing. He has joined in the group of Professor Caofeng Pan at Beijing Institute of Nanoenergy and Nanosystems, Chinese Academy of Sciences as a visiting student since 2013. His research interests mainly focus on the synthesis of organic-inorganic hybrid perovskite and their application in photoelectric devices.



Xun Han received his undergraduate degree from Shandong University in 2012. Currently he is pursuing his Ph.D. under the supervision of Prof. Caofeng Pan at Beijing Institute of Nanoenergy and Nanosystems, Chinese Academy of Sciences. His research is mainly focused on piezotronics and piezo-phototronics and their applications in human-electronics interfacing.



Dr. Chuntao Liu received his B.S. (1987) and M.S. degree (1993) in Mechanics from the Beijing University and Xi'an Jiaotong University, respectively, and received his Ph.D. (2003) in Materials Processing Engineering from Zhengzhou Univ.. He was visiting scholar at Ohio State University during 2006–2007. He is currently a professor in National Engineering Research Center for Advanced Polymer Processing Technology, Zhengzhou University. His research focuses on the fields of advanced multifunctional polymer materials.

Movie S1. Real-time response of the device to the phonations of “One World One Dream” with a piece of music as background noise by attaching it on the neck of the volunteer.

Movie S2. Real-time response of the device to the phonations of “Sensor” with a piece of music as background noise by attaching it on the neck of the volunteer.



Dr. Changyu Shen, the academician, director of National Engineering Research Center for Advanced Polymer Processing Technology, was born at Nanyang, Henan, in 1963. He received his PhD from Dalian University of Technology in 1990, and then joined Zhengzhou University. He was promoted to a full professor in 1993. His research focuses on polymer nanocomposites, computer aided engineering for polymer processing and biomimetic polymer materials.

Movie S3. Real-time response of the device to the phonations of “Zhengzhou University” with a piece of music as background noise by attaching it on the neck of the volunteer.



Dr. Lin Dong received his B.S. (1998) and M.S. degree (2001) in Chemistry from Jilin University, and the Ph.D. degree (2005) in Condensed Matter Physics from Changchun Institute of Optics, Fine Mechanics and Physics, Chinese Academy of Sciences. He then joined Zhengzhou University. He is currently a professor in School of Physics & Engineering, Zhengzhou University. His research focuses on the fields of spectroscopic properties and piezotronic/piezophototronic effects of nano-devices.



Dr. Jin Yang received the B.E., M.E. and Ph.D. degrees in instrumentation science and technology from Chongqing University in 2002, 2004, and 2007, respectively. Currently, he is a professor with the College of Optoelectronic Engineering, Chongqing University. His current research interests focus on sensor and actuator, measurement and instrumentation, nanogenerator, self-powered sensor and systems.



Dr. Caofeng Pan received his B.S. degree (2005) and his Ph.D. (2010) in Materials Science and Engineering from Tsinghua University, China. He then joined the Georgia Institute of Technology as a postdoctoral fellow. He is currently a professor and a group leader at Beijing Institute of Nanoenergy and Nanosystems, Chinese Academy of Sciences since 2013. His main research interests focus on the fields of piezotronics/piezo-phototronics for fabricating new electronic and optoelectronic devices, nano-power source (such as nanofuel cell, nano biofuel cell and nanogenerator), hybrid nanogenerators, and self-powered nanosystems. Details can be found at <http://piezotronics.binnccas.cn/index%20en.php>.